Measurements of Beat-Wave-Accelerated Electrons in a Toroidal Plasma

J. H. Rogers[a] and D. Q. Hwang

Department of Applied Science, University of California at Davis, Davis, California 95616
and Lawrence Livermore National Laboratory, Livermore, California 94550

(Received 23 January 1992)

Electrons are accelerated by large amplitude electron plasma waves driven by counterpropagating microwaves with a difference frequency approximately equal to the electron plasma frequency. Energetic electrons are observed only when the phase velocity of the wave is in the range $3v_e < v_{ph} < 7v_e$ (v_{ph} was varied $2v_e < v_{ph} < 10v_e$), where v_e is the electron thermal velocity, $(kT_e/m_e)^{1/2}$. As the phase velocity increases, fewer electrons are accelerated to higher velocities. The measured current contained in these accelerated electrons has the power dependence predicted by theory, but the magnitude is lower than predicted [B. I. Cohen *et al.*, Nucl. Fusion **28**, 1519 (1988)].

PACS numbers: 52.35.Mw, 52.25.Sw, 52.35.Nx, 52.55.Fa

Noninductive current drive has been an important aspect of tokamak research for many years. Although several approaches have been advanced, none is ideal. One approach which has received theoretical and computational consideration, but has not been experimentally demonstrated, is beat-wave current drive [1]. This current drive scheme uses copropagating or counterpropagating electromagnetic waves with a difference in frequency approximately equal to electron plasma frequency to drive large amplitude electron plasma waves via the nonlinear $\mathbf{v}(\omega_0,k_0)\times\mathbf{B}(\omega_1,k_1)$ force [2]. Energy and momentum of the electrostatic plasma wave is then transferred to the electrons by either Landau damping or trapping, resulting in a high-energy tail in the electron velocity distribution in the direction of $\mathbf{k}_e$. In order for the driven wave to stay in phase with the driving force, $\omega_e=\omega_0-\omega_1$ and $\mathbf{k}_e=\mathbf{k}_0-\mathbf{k}_1$. Thus, the phase velocity of the electron plasma wave is $v_{ph}=(\omega_0-\omega_1)/|\mathbf{k}_0-\mathbf{k}_1|$ which results in a much larger phase velocity wave for copropagating electromagnetic waves than counterpropagating waves. For the counterpropagating electromagnetic waves, the growth rate of the electrostatic plasma waves is larger, and the coupling to the electrons is stronger because of the lower phase velocity.

There has been no previous experimental testing of beat-wave current drive primarily because of the lack of very high intensity millimeter wave sources which are necessary to achieve high current drive efficiency in a tokamak [3]. In the experiment described below, counterpropagating microwaves were launched in a toroidal plasma with only a toroidal magnetic field and no initial plasma current. Electrostatic plasma waves are measured to grow linearly in time and then saturate [4]. Accelerated electrons are measured with an electrostatic energy analyzer. The current drive efficiency is low in this experiment, but because of the low electron temperature, the low plasma density, and lack of any initial current, the effects are measurable.

The measurements are performed in the Davis Diverted Torus (DDT) operating in a low density (7×10^7–2×10^9 cm^{-3}), high repetition rate (15 shots/sec) mode. In this mode, a low-level steady-state toroidal magnetic field is used ($B\sim110$ G). DDT is a toroidal device with a major radius of 45 cm and a minor radius of 15 cm. A pulsed, hot tungsten wire cathode (-150 V, 300 μsec) emits primary electrons which partially ionize the argon gas at a pressure of approximately 1×10^{-4} torr (base pressure $\sim2\times10^{-7}$ torr). The experiments are performed 30 μsec after the discharge pulse when the primary electrons have left the system and the electrons have a Maxwellian velocity distribution with a temperature of ~1 eV. Two microwave beams are then launched in opposing directions (see Fig. 1). The microwave pulses have a duration of 400 nsec with peak powers of ~200 kW. The density is changed by varying the emission current of the hot cathode by changing the heating current through the filament. This approach is taken to minimize changes in the electron temperature and density profile. Because there is only a toroidal magnetic field, the profile is not symmetric in the poloidal direction. An additional vertical magnetic field improved the symmetry of the poloidal density profile but increased the toroidal density gradient. The configuration with no vertical magnetic field was found to couple energy to the electrons more efficiently.

The microwaves are generated by two tunable magnetrons with a frequency range 8.5 to 9.5 GHz and peak

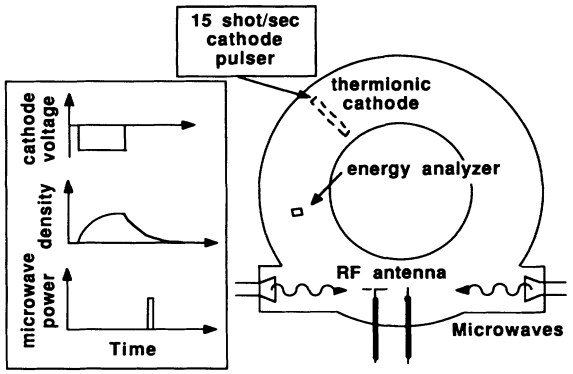

FIG. 1. A schematic drawing of the beat-wave experiment on the Davis Diverted Torus (DDT).

power $\lesssim 200$ kW for a 400-nsec pulse. The microwave power level is adjusted by using high power microwave attenuators in order to avoid the frequency shift that results from changing the high voltage amplitude on the magnetron oscillators. In order to minimize cavity modes, the walls of the interaction region are lined with microwave absorbing tiles. Tile baffles are also used around the microwave horns to reduce interference in the microwave profile caused by reflections from the wall near the horn.

The plasma diagnostics used consisted of cylindrical Langmuir probes and an electrostatic energy analyzer. The cylindrical Langmuir probes were used to measure the initial electron temperature, plasma potential, density, and the electrostatic wave driven by the microwaves. The current versus probe voltage (IV) characteristic was obtained using a computer-controlled system which relied on the shot-to-shot reproducibility of the plasma (which was found to be excellent). The probe was biased by the output of an amplifier which is controlled by a digital to analog converter output from a DEC LSI 11/73 computer. On a given shot, one measurement of the probe current and voltage is taken at a specific time relative to the plasma decay using a track and hold circuit and the analog to digital converter in the computer. The probe voltage was then incremented for the next shot.

The electrostatic energy analyzer is used to measure the tail of the electron velocity distribution. The energy analyzer uses the same control circuitry as the Langmuir probe, except the second grid voltage is swept and measured and the current to the collector (biased ~ 15 V) is measured. The first grid is grounded. At the time the microwaves are triggered, the plasma temperature is ~ 1 eV. In order to further minimize the perturbation to the plasma caused by the presence of the energy analyzer, the aluminum body of the analyzer has been anodized to make the surface nonconductive. Therefore the surface will remain at the floating potential and reflect most electrons, while the aluminum body shields the diagnostic screen and collector from the microwaves. The plasma potential measured by the Langmuir probe is consistently measured to be ~ 4 V higher than the energy analyzer measurement, and the initial electron temperature measured with the Langmuir probe is ~ 1 eV whereas the energy analyzer measures ~ 2 eV. This is believed to be caused by the particle depletion on the magnetic field lines that intersect the energy analyzer. Sugawara [5] developed a theory on this effect which, for our parameters, would predict a difference of ~ 3 V. However, Sugawara estimates the plasma potential using the intersection of the electron saturation current and the retarded electron current versus voltage, which will overestimate the plasma potential [6] thereby underestimating the change in plasma potential.

Monitoring the electrostatic wave energy, it is found that waves are driven when $\omega_{pe} \geq \omega_e$ $(=\omega_0 - \omega_1)$ [4]. Modes for which $\omega_e < \omega_{pe}$ are bounded plasma modes with long wavelength (high phase velocity) [7]. Electrons are only accelerated at a single density ($\pm 15\%$) by the lowest phase velocity waves excited, i.e., those with wavelengths much shorter than the dimensions of the vacuum vessel which approximately follow the Bohm-Gross dispersion relation [4]. The accelerated electrons are measured after a time delay approximately equal to the propagation time between the interaction region and the position of the energy analyzer for a particle traveling at the phase velocity of the wave. Because of this propagation delay, the bulk of the energetic electron signal is measured after the microwaves have turned off [4]. There is no energetic electron tail observed when the energy analyzer is turned to face away from the interaction region, or when either microwave source is turned off.

Two typical energy analyzer measurements taken ~ 100 nsec after the end of the microwave pulse are shown in Fig. 2. The measured energy analyzer current [(a) and (c)] is differentiated with respect to the bias voltage in order to obtain the energy distribution function [(b) and (d)]. The energy distribution function is then integrated (to check the differentiation) and displayed as solid lines in Figs. 2(a) and 2(c). As seen in these two examples, electrons are accelerated from velocities below the phase velocity of the wave to velocities well beyond the phase velocity of the wave. Also, for higher phase velocity waves, fewer electrons are accelerated to higher energies. In order to illustrate this point further, Fig. 3 shows the extent of the energetic electron tail for different phase velocities. Here, the extent of the tail is defined as follows: The low-energy limit is the energy at which the modified distribution deviates from the initial Maxwellian distribution (circle), and the high-energy limit is energy at which the distribution function drops approximately one e-fold from the maximum value in the tail (square). These limits are illustrated in Figs. 2(b) and 2(d). As shown in Fig. 3, the range of energies approximately increases linearly with the phase velocity. The highest phase velocity point in Fig. 3 differs from the others because, in addition to the energetic tail, there appeared to be some coupling to the bulk electrons so the modified distribution deviated from the initial distribution at a lower energy.

An analytical estimate of the coupling efficiency of the beat wave process has been made by Kaufman and Cohen [8]. These calculations were performed using the wave action flux, $\mathbf{J}_i$, from which the energy density flux, $\omega_i \mathbf{J}_i$, and the momentum density flux, $k_i \mathbf{J}_i$, of the electromagnetic or electrostatic wave can be defined. For electromagnetic waves,

$$\mathbf{J}_i = (m_e c^2/e)^2 (\mathbf{k}_i/2\pi) |u_i/c|^2 ,$$

where u_i is the electron oscillation velocity, $eE_i/m\omega_i$. Action flux is a conserved quantity (conservation of energy and momentum), so the reduction in action flux in the high frequency electromagnetic wave is equal to the increase in action flux in the electrostatic wave and the

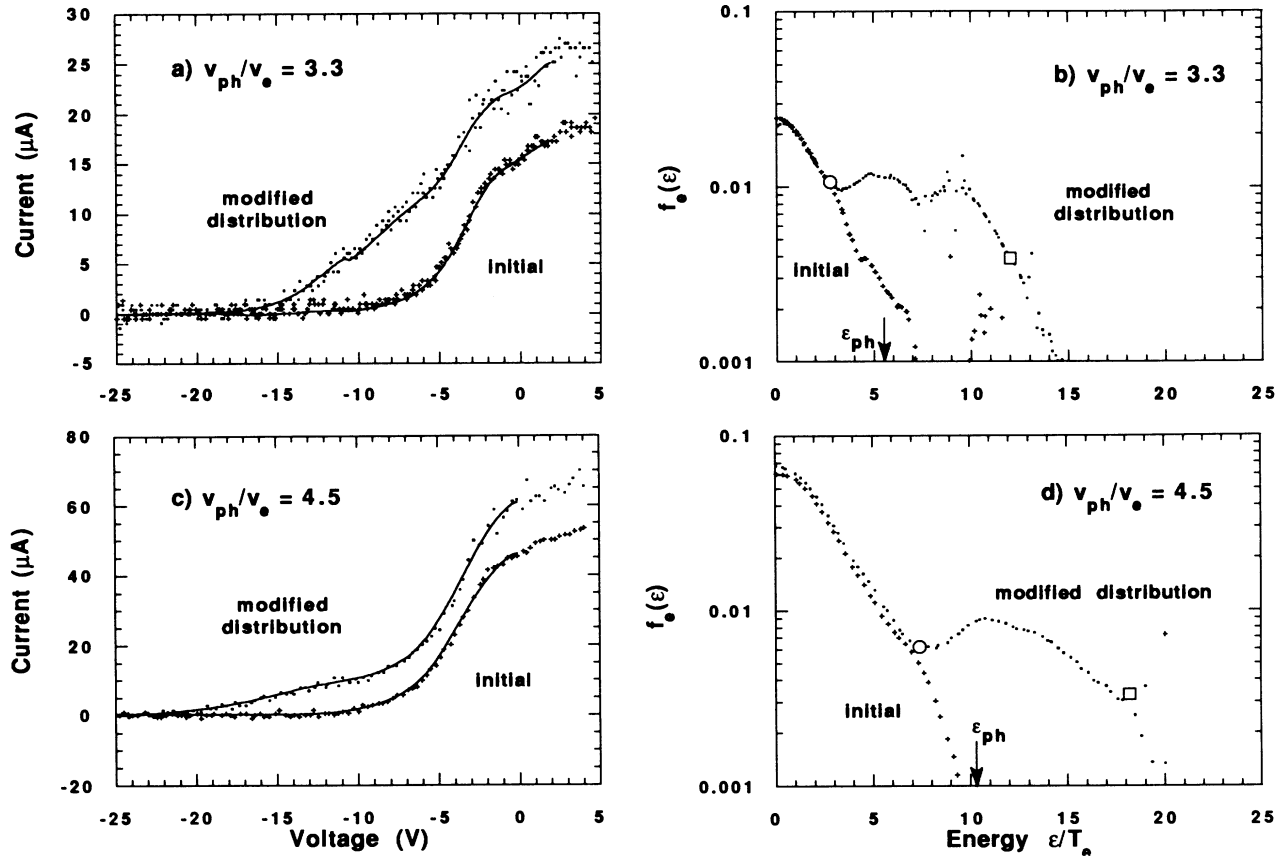

FIG. 2. Typical energy analyzer data are shown for $v_{ph}/v_e = 3.3$ [(a) and (b)] and $v_{ph}/v_e = 4.5$ [(c) and (d)]. The raw data [(a) and (c)] are differentiated in order to give the distribution function [(b) and (d)]; this result is then integrated to verify the differentiation [lines in (a) and (c)]. The circle and square in (b) and (d) are examples of the upper and lower limits of the accelerated electron tail. Note also that the energies marked in (b) and (d), ε_{ph}, are the kinetic energies of an electron traveling at the phase velocity of the wave.

low frequency electromagnetic wave, i.e., $\omega_0 \Delta J = \omega_1 \Delta J + \omega_e \Delta J$. Kaufman and Cohen derived the following result for the coupling efficiency of the beat-wave process for counterpropagating electromagnetic waves:

$$\bar{J}_0 \equiv \left(\frac{k_e^2}{k_0 k_1}\right) \pi k_0 L \left|\frac{u_0^{\text{in}}}{c}\right|^2$$
$$= (1 - R_a - \rho)^{-1} \ln[(1 - R_a)(\rho + R_a)/\rho] ,$$

where L is the density scale length along the toroidal direction (the gradient is assumed to be linear), R_a is the relative action transfer $\Delta J / J_0^{\text{in}}$, and ρ is the relative amplitude of the electromagnetic waves $u_1^{\text{in}}/u_0^{\text{in}}$. In the limit relevant to this experiment, $R_a \ll 1$, with $\rho \sim 1$ the above relationship reduces to $R_a \sim \rho \bar{J}_0$. Simulation results indicate that when the plasma wave phase velocity is less than $\sim 7.5 v_e$, the momentum in the wave is efficiently coupled to the electrons [3]. Consistent with the simulation results, energetic electrons were only measured when $v_{ph} < 7 v_e$, although electrostatic waves were measured at higher phase velocities. If all the momentum in the electrostatic wave is transferred to the electron distribution,

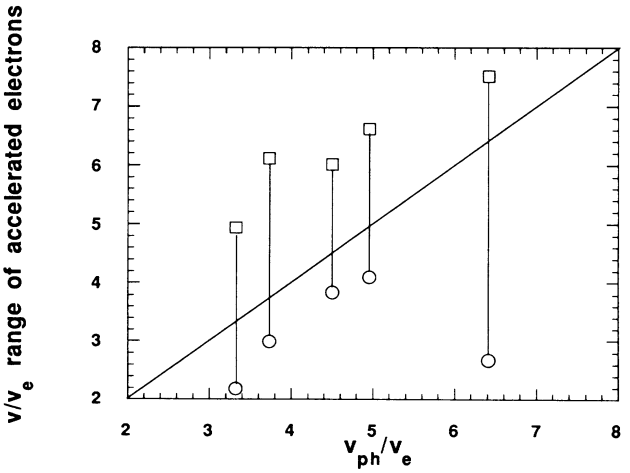

FIG. 3. The range in velocity of the accelerated tail of electrons is shown vs the phase velocity (both normalized to the thermal velocity). The low-energy limit is determined by where the modified distribution function deviates from the initial distribution, and the high-energy limit is defined as where the amplitude drops approximately one e-fold from the maximum value in the tail.

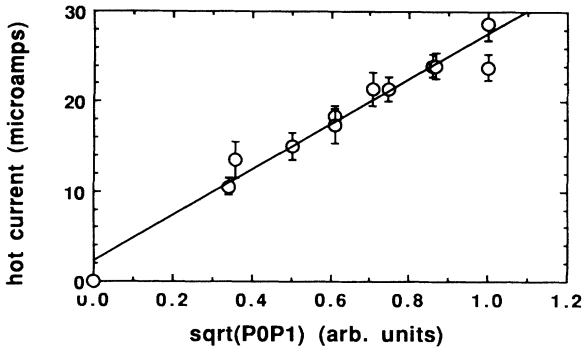

FIG. 4. The total hot electron current is shown vs $(P_0P_1)^{1/2}$. The error bars are 1 standard deviation of measurement at several voltages near the plasma potential. The line is a least-squares fit to the data.

the resulting current density is

$$en_e\langle v\rangle = \frac{m_e\omega_{pe}}{e}\left[\frac{c}{8\pi}\frac{\omega_0(\omega_0+\omega_1)^3}{\omega_1}L\right]^{1/2}\left|\frac{u_0^{\rm in}}{c}\right\|\frac{u_1^{\rm in}}{c}\Big| \propto (I_0I_1)^{1/2},$$

where I_i is the intensity of the ith wave.

Figure 4 shows the power dependence of the accelerated electron current. The accelerated electron current is given by measuring the difference in current on the energy analyzer with and without the beat wave excited at bias voltages near the plasma potential. The linear dependence of the current on $(P_0P_1)^{1/2}$ is verified. In the present experiment, the toroidal geometry is expected to dominate the effective density gradient scale length [9], L (the toroidal density scale length is $\sim$300 cm). Because the theory is one dimensional, a direct comparison of the predicted current drive efficiency to the experiment is difficult. Even if an effective scale length of $L\sim5$ cm is used, the measured current density is of the order 3 to 10 times smaller than that predicted by the above theory. One possible explanation for this discrepancy is that the group velocity of the wave in a bounded plasma is somewhat higher than an infinite plasma [4], which is assumed in the theory, so the waves will propagate through the resonant region more quickly and therefore grow to a smaller amplitude. Also, the energy analyzer may be too close to the interaction region to allow the waves sufficient time to damp.

Even though these experiments are performed in a low efficiency regime (low microwave intensity and $\omega_{0,1}\gg\omega_e$) a significant modification to the tail of the electron distribution function is obtained (Fig. 2). The ability to produce a high-energy tail may have additional benefits for tokamak operation besides the current directly driven. It may be of use in conjunction with other current drive techniques, or in seeding a bootstrap current [10]. The important contribution which beat-wave acceleration of electrons may add is that the current profile may be chosen to improve stability and confinement.

This research has been supported by U.S. Department of Energy Contract No. DE-FG03-89ER53289, the Plasma Physics Research Institute of LLNL, and the Department of Applied Science of the University of California at Davis. The authors are also grateful for the useful discussions with G. Dimonte, B. I. Cohen, and J. Killeen and the technical support of Ted Hillyer.

[a]Permanent address: Princeton Plasma Physics Laboratory, Princeton, NJ 08543.

[1] V. Stefan, B. I. Cohen, and C. Joshi, Science **243**, 494 (1989).

[2] M. N. Rosenbluth and C. S. Liu, Phys. Rev. Lett. **29**, 701 (1972).

[3] B. I. Cohen, R. H. Cohen, B. G. Logan, W. M. Nevins, G. R. Smith, A. V. Kluge, and A. H. Kritz, Nucl. Fusion **28**, 1519 (1988).

[4] J. H. Rogers, D. Q. Hwang, J. C. Thomas, R. L. Horton, J. Killeen, and G. Dimonte, Phys. Fluids B **4**, 1920 (1992).

[5] M. Sugawara, Phys. Fluids **9**, 797 (1966).

[6] J. H. Rogers, J. S. De Groot, and D. Q. Hwang, Rev. Sci. Instrum. **63**, 31 (1992).

[7] A. W. Trivelpiece and R. W. Gould, J. Appl. Phys. **11**, 1784 (1959).

[8] A. N. Kaufman and B. I. Cohen, Phys. Rev. Lett. **30**, 1306 (1973).

[9] M. R. Amin and R. A. Cairns, Nucl. Fusion **30**, 327 (1990).

[10] J. A. Heikkinen, S. J. Karttunen, and R. R. E. Salomaa, Nucl. Fusion **28**, 1845 (1988).